

QUANTIFICATION OF SHOCK STAGES IN UREILITE OLIVINE BY *IN-SITU* MICRO X-RAY DIFFRACTION

Y. Li^{1,2}, P.J.A. McCausland^{1,2}, and R.L. Flemming^{1,2}. ¹Department of Earth Sciences and ²Centre for Planetary Science and Exploration (CPSX), Western University, London, ON, Canada N6A 5B7. yli2889@uwo.ca

Introduction: Ureilites consist mainly of olivine and pyroxene, high abundances of carbon phases such as graphite or diamond, and accessory phases such as metals and sulfides [1,2]. Ureilites appear to have undergone multiple melting and cooling events, with plagioclase being completely precipitated out or removed during the processing [1]. However, by comparison with other achondrites, ureilites have high abundances of trace siderophile elements, suggesting that extensive differentiation processes involving metal segregation have not occurred [1]. It has been proposed that all ureilites have been through some possibly complex shock histories [2], however currently there is no rigorous assessment for ureilitic shock classification.

In this study, we use *in situ* micro X-ray diffraction to examine olivine deformation for ureilite meteorites Elephant Moraine 96042, Shişr 007, Northwest Africa 7059, Allan Hills A 81101, Larkman Nunatak 04315 and Elephant Moraine 88720. Raman spectroscopy was also used to investigate the phase identity of silicates and carbonaceous dark matter as an additional constraint on peak shock pressures in a slab sample of Shişr 007.

Method: Micro X-ray diffraction (μ XRD) provides a method for *in situ* examination of rock samples with a range of surfaces, from irregular fractures to cut surfaces and polished thin sections or probe mounts [3]. This study used the Bruker D8 Discover μ XRD at Western University with a Co K α X-ray source ($\lambda = 1.78897$ Å) and General Area Detector Diffraction System (GADDS) which obtains 2D diffraction patterns similar to Debye-Scherrer film (Fig. 1). Strained minerals exhibit streaks in these diffraction patterns on GADDS images, which lie along the arc of Debye rings, or chi direction (χ) for each lattice plane with Miller index (hkl). XRD data for all samples was collected by omega scan mode. To maximize collecting area, we used $\theta_1 = 14.5^\circ$, $\theta_2 = 20.5^\circ$ and $w = 10^\circ$ for Frame 1; $\theta_1 = 37^\circ$, $\theta_2 = 43^\circ$ and $w = 16^\circ$ for Frame 2. For each frame, we collected 1 hour, making 2 hours per target.

Measurements of the full width at a half maximum along the Debye rings (FWHM_χ) provide a quantitative index of crystal strain-related mosaicity or misorientation of subdomains or ‘mosaic blocks’ in a single crystal due to non-uniform strain (plastic deformation) [4,5,6]. For any given analysis location, multiple lattice planes are chosen to make the measurements of FWHM_χ [4, 7]. In case of measuring FWHM_χ for ‘complex’ asymmetrical or multiple peaks and comparing of results from ‘simple’ peak EVA software-based analysis, we developed Matlab codes that are based on a conventional Lorentzian function to best fit peaks and measure the sum of FWHM_χ for individual peaks

($\sum_n(\text{FWHM}_{\chi_n})$). For Shişr 007, as it is a slab sample, we used micro-Raman spectroscopy with laser beam $\lambda = 532$ nm at Western University Yang Song Research Laboratory before μ XRD to identify olivine and pyroxene mineral phases, and possible carbonaceous minerals for petrographic study.

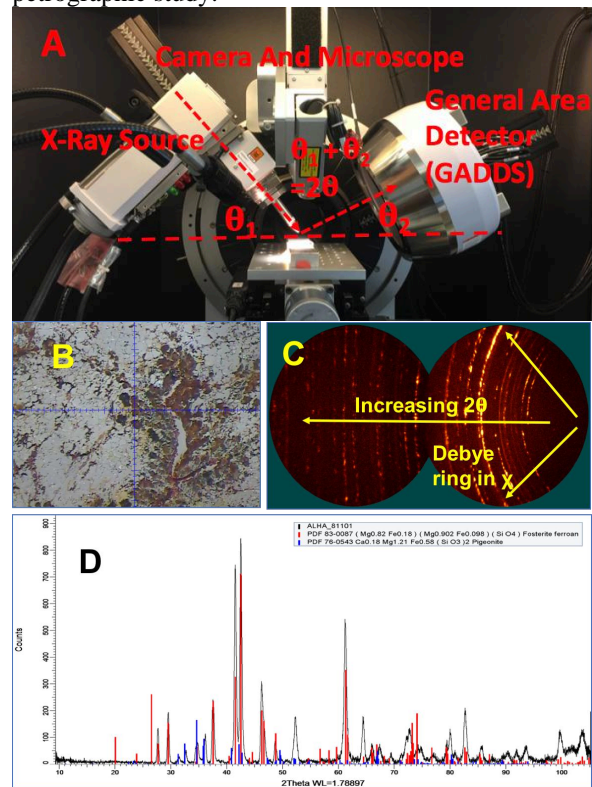


Figure 1A *in situ* micro X-ray diffraction geometry; **1B** to **1D** shows a portion of the highly shocked ureilite ALHA 81101 with shattered polycrystalline olivine (**1B**; image width 2 mm), and its 2D diffraction pattern GADDS image with ‘spotty rings’ (**1C**) and integrated intensity versus 2θ diffraction pattern allowing for phase identification (**1D**).

Results: Data collection for sample EET 96042, Shişr 007, NWA 7059, ALHA 81101 and LAR 04315 has been done, among which, complete data analysis (including both EVA and best fit sum) for EET 96042, Shişr 007 and NWA 7059 are done (see Fig. 2). We collected multiple olivine lattice planes for comparison.

EET 96042 was classified as weakly shocked non-brecciated ureilite sample as olivine shows weak undulatory extinction in thin section. It is carbon-rich with a trace amount of metal and troilite [8]. Lattice (021) is the most common lattice plane for this sample ($n = 14$) following by (131) ($n = 12$) and (122) ($n = 11$). FWHM_χ for (021) is 2.32 ± 1.07 by EVA, and 4.33 ± 1.38 by best fit sum; FWHM_χ for (131) is 2.44 ± 0.85 by EVA, and

4.96 ± 1.83 by best fit sum. FWHM_χ for (122) is 1.87 ± 0.59 by EVA, and 3.71 ± 1.09 by best fit sum.

Shiřr 007 was classified as moderate shocked non-brecciated ureilite, and olivine grains show mosaicism. It is carbon-rich, and carbonaceous matter commonly occurs as narrow intergranular veins [9]. Raman spectroscopy showed the sample has the possibility to have micro diamond or carbon-lonsdaleite-diamond system in the carbon matter. Lattice (112) is the most common lattice plane for this sample ($n=14$) following by (021) ($n=8$) and (111) ($n=7$). FWHM_χ for (112) is 3.01 ± 1.65 by EVA, and 4.83 ± 2.54 by best fit sum; FWHM_χ for (021) is 1.94 ± 0.60 by EVA, and 3.77 ± 1.35 by best fit sum. FWHM_χ for (111) is 2.00 ± 1.14 by EVA, and 3.65 ± 1.92 by best fit sum.

NWA 7059 is a slab sample as well. It is also considered as a moderate shocked ureilite by undulatory extinction on olivine grains [10]. Lattice (112) is the most common lattice plane for this sample ($n=6$) following by (122) ($n=3$) and (130) ($n=3$). FWHM_χ for (112) is 2.42 ± 1.32 by EVA, and 4.50 ± 1.52 by best fit sum; FWHM_χ for (122) is 1.38 ± 0.38 by EVA, and 2.66 ± 0.45 by best fit sum. FWHM_χ for (130) is 1.79 ± 0.88 by EVA, and 5.62 ± 1.78 by best fit sum.

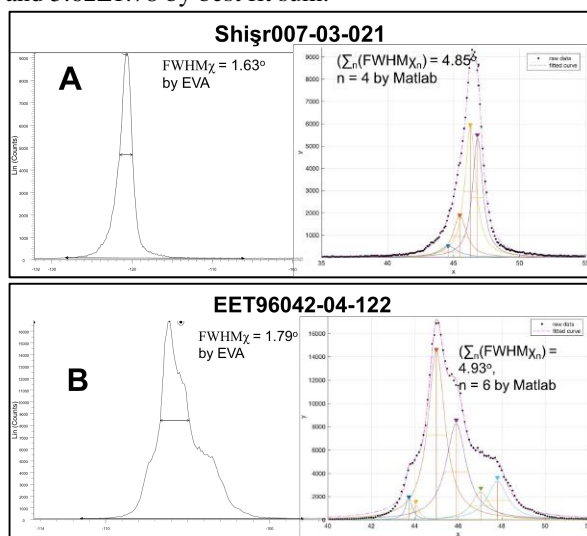


Figure 2. Peak fitting in Matlab for different asymmetrical peaks. **Figure 2A** is showing results for peak with higher symmetry for Shiřr 007, target 3 and lattice plane (021); left is result by EVA with $\text{FWHM}_\chi = 1.63^\circ$ and right is result by Matlab with $\sum_n(\text{FWHM}_{\chi_n}) = 4.85^\circ$, $n = 4$, $R^2 = 0.999$ and $\text{RMSE} = 66.28^\circ$. **Figure 2B** shows an asymmetrical peak for EET96042, target 4, and lattice plane (122); left is result by EVA with $\text{FWHM}_\chi = 1.79^\circ$ and right is result by Matlab with $\sum_n(\text{FWHM}_{\chi_n}) = 4.99^\circ$, $n = 6$, $R^2 = 0.997$ and $\text{RMSE} = 262^\circ$.

LAR 0413 and ALHA 81101 are highly shocked ureilites. Olivine grains in LAR 04315 show strong mosaicism. Some of the subgrains are misorientated whereas some have similar orientations. All olivine grains in ALHA 81101 have been shattered to become

polycrystalline; the original grain boundaries are rimmed and still identifiable. Pyroxenes show strong undulatory extinction with blade shape graphite inclusion (Fig. 3). GADDS images show “spotty rings” (Fig. 1 and 4C), and peaks are much longer than those from previous lower shocked meteorites (Fig. 4A). As of this writing, data from these more highly shocked meteorites need further analysis for shock comparison.

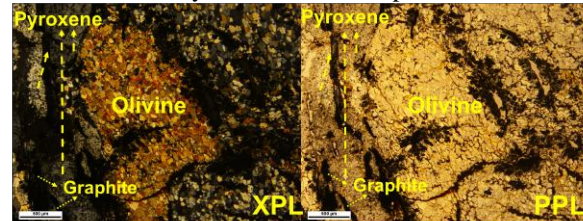


Figure 3. Thin section of ALHA 81101, left is under XPL and right is under PPL. As on diagram, olivine has rimmed grain boundaries and polycrystalline textures and pyroxene is showing undulatory extinction.

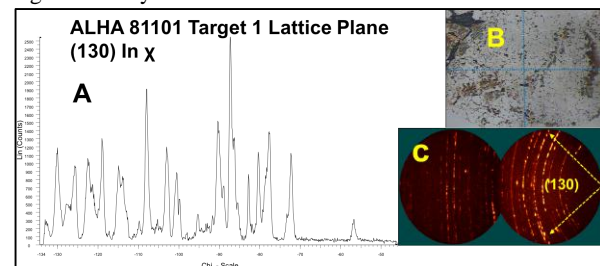


Figure 4. Example of peaks in χ for lattice plane (130) in ALHA 81101 Target 1. **Fig. 4A** is the peaks that are intergraded in χ ; **Fig. 4B** is the targeting image and **Fig. 4C** is GADDS image. Peaks are much longer compared to the previous lower shocked examples (as shown in Fig. 2A and 2B).

References [1] Goodrich C.A. (1992) *Meteoritics*, 27: 327–352; [2] Rubin, A. E. (2006). *Meteoritics & Planetary Science*, 41(1), 125-133; [3] Flemming R.L. (2007) *Canadian Journal of Earth Sciences*, 44: 1333–1346; [4] Vinet N. et al. (2011) *American Mineralogist*. 96 (4): 486-497; [5] Hörz F. and Quaide W. (1973) *Earth, Moon, and Planets*, 6: 45–82; [6] Klug H.P. and Alexander L.E. (1962) *X-ray diffraction procedures*, 3rd ed: p716; [7] Izawa M.R.M. et al. (2011) *Meteoritics & Planetary Science*, 46 (5): 638-651. [8] McCoy T. (1998) *Meteoritical Bulletin*, no. 82, MAPS 33, A221-A240; [9] Wlotzka F. and Bartoschewitz R. (2002) *Meteoritical Bulletin*, no. 86, MAPS 37, A157-A184; [10] Irving A. and Kuehner S. (2015) *Meteoritical Bulletin*, no. 102, MAPS 50, 1662.

Acknowledgements: We thank the Royal Ontario Museum and the Antarctic Meteorite program via NASA JSC for providing several ureilite samples on loan. Alex Rupert assisted with XRD training. Dr. Yang Song provided Raman instruments and helped with data collection. Fengke Cao advised on Raman spectroscopy.